8. Neutronics Analyses for the Spallation Neutron Source Second Target Station

Igor Remec, Franz X. Gallmeier, Mark J. Rennich, Thomas J. McManamy, Irina Popova, Wei Lu
Oak Ridge National Laboratory, Oak Ridge, United States

Abstract

The Spallation Neutron Source (SNS) and the High Flux Isotope Reactor (HFIR), two of the word-class neutron scattering facilities, are located at the Oak Ridge National Laboratory. The SNS and HFIR are funded by the U.S. Department of Energy, Office of Science, Office of Basic Energy Science, and are operated as user facilities, available to researchers from all over the world. Currently there are 13 neutron scattering instruments in operation at the HFIR and 20 at the SNS First Target Station.

Producing the cutting edge science requires continuous improvements and development of the facilities and instruments. The SNS was designed from the beginning to allow addition of the second target station (STS) and an upgrade of the accelerator power. At this time both advances: the accelerator upgrade and the construction of the STS are in preparation.

Current baseline design for the STS calls for a rotating compact tungsten target. The target station is driven with short (<1 µs) proton pulses at 10 Hz repetition rate and 467 kW proton beam power, and is optimised for high intensity and high resolution long wavelength neutron applications. The proton beam footprint as small as acceptable from the mechanical and heat removal aspects is planned to generate a compact-volume neutron production zone in the target, which is essential for tight coupling of the target and the moderators and for achieving high-intensity peak thermal and cold neutron fluxes. The STS will allow operation of approximately 22 beamlines and will expand and complement the current national neutron scattering capabilities.

This paper will present an update of the status of the neutronics analyses performed for the STS and will discuss the performance of the moderators, heating rates, activation analyses and shielding calculations which provide input in the engineering design.

8.1. Introduction

The Spallation Neutron Source (SNS) is in operation at the Oak Ridge National Laboratory since 2006. It provides the most intense pulsed neutron beams in the world for scientific research and industrial development. SNS is funded by the US Department of Energy, Office of Science, Office of Basic Energy Science, and is operated as user facility, available to researchers from all over the world. Currently 20 state-of-the-art neutron scattering instruments are in operation at the SNS and provide a variety of capabilities for researchers across a broad range of disciplines, such as physics, chemistry, materials science and biology.

Producing cutting edge science requires continuous improvements and development of the facilities and instruments. The SNS was designed from the beginning to allow addition of the second target station (STS) and an upgrade of the accelerator power. At this time both advancements: the accelerator upgrade and the construction of the STS are in preparation.

8.1.1. STS target/moderator/reflector design

The current baseline design for the STS calls for a rotating compact tungsten target. The target station is driven with short (<1 μs) proton pulses at 10 Hz repetition rate and 467 kW proton beam power, and is optimised for high intensity and high resolution long wavelength neutron applications. The proton beam footprint is as small as acceptable from the mechanical and heat removal aspects in order to generate a compact-volume neutron production zone in the target, which is essential for tight coupling of the target and the moderators and for achieving high-intensity peak thermal and cold neutron fluxes. Selected parameters of the STS and the first target station (FTS) after the upgrade of the accelerator power are presented in Table 8.1.

Table 8.1. Selected FTS and STS parameters

First target station (Upgraded)	Second target station
Short (<1 s) proton pulses	Short (<1 s) proton pulses
1.3 GeV protons	1.3 GeV protons
50 Hz repetition rate	10 Hz repetition rate
2 MW beam power	467 kW beam power
40 kJ per proton pulse	47 kJ per proton pulse
Large beam footprint ; ~ 140 cm^2	Small beam footprint ; ~ 30 cm^2 (90% of the beam)
Mercury target	Tungsten target, (Tantalum clad, D_2O cooled)

Three moderators are currently planned for the STS that will allow operation of approximately 22 beamlines and will expand and complement the current national neutron scattering capabilities. A high peak brightness cylindrical coupled para-H_2 moderator, with two 3 cm x 3 cm viewed faces and one 3 cm x 6 cm viewed face, is placed above the target. The high-intensity box-shaped coupled para-H_2 moderator with a 5 cm x 5 cm face area viewed from one side is placed in the upstream position below the target. Finally, a multi-spectral decoupled moderator with two 7 cm x 7 cm viewed faces and cadmium poison plate separating the two moderator volumes is placed in the downstream position below the target. The thermal face of this moderator is viewing H_2O at ambient temperature, and the cold face is viewing liquid para-H_2. The decoupled moderator has the moderator vessel coated with cadmium absorber except for the viewed areas to prevent crossing of thermal neutrons from the reflector into the moderator for sharpening the emitted neutron pulse time structure. At coupled moderators such absorber layers are absent.

The inner reflector plug will be water-cooled beryllium and the outer reflector region will be water-cooled stainless steel SS-316; it has not been decided yet if heavy water will be used.

8.2. Moderator performance

The comparison of the peak brightness of the coupled para-H_2 moderators for the rotating STS configuration and the previously considered stationary target configuration [1] are shown in Figure 8.1, along with the brightness for the FTS beamline 5 (BL5, light blue solid line curve) which views the top downstream coupled para-H_2 moderator. Along with the STS stationary target results for the cylindrical moderator (solid line curves: red for the first 3 cm x 3 cm viewed area, green for the second 3 cm x 3 cm viewed area, and dark blue for the 3 cm x 6 cm viewed area), the curve for the high-intensity box-shaped moderator with viewed area 5 cm x 5 cm (pink curve) is also shown. The curves for the same set of moderators on the rotating target are shown with the set of dot-dashed lines (yellow, blue, red and grey). The results for the STS are normalised to 467 kW proton beam power and 10 Hz pulse repetition rate, while the results for the FTS are normalised for 2 MW beam power and 50 Hz repetition rate. Figure 8.2 depicts the ratio of the peak brightness of the STS coupled para-H_2 moderator with 3 cm x 3 cm viewed area (solid red line), and the STS coupled para-H_2 moderator with 5 cm x 5 cm viewed area (solid green line), to the peak brightness of the FTS BL5. The dot-dashed red and green lines depict the same comparison for the rotating STS configuration.

The coupled para-H_2 moderator peak brightness for the STS is about 10 to 14 times higher than the brightness for the FTS coupled moderators in the range below 10 meV. The STS gains with respect to the FTS were obtained by moving the coupled H_2 moderators to the prime neutron production zone of the target, by having a moderator depth optimised for para-hydrogen, and by reducing target and moderator dimensions and improving the target-moderator coupling. Another factor contributing to the higher brightness of STS moderators are smaller viewed areas which are 5 cm x 5 cm (top upstream moderator), and 3 cm x 6 cm and 3 cm x 3 cm (bottom moderator) for the STS, and 10 cm x 12 cm for the FTS. The rotating and stationary STS configurations deliver very similar coupled para-H_2 moderator peak brightness, with a slight advantage on the side of rotating target.

The peak brightness for the STS decoupled para-H_2 and ambient temperature H_2O moderators is shown in Figure 8.3, together with the brightness for the FTS para-H_2 (BL2) and H_2O (BL17) decoupled moderators. For the STS the results are given for the rotating and stationary target configuration. The STS decoupled moderator placement is restricted to the location downstream of the coupled moderator. This results in ~25 % reduction in decoupled para-H_2 moderator performance with respect to an optimally placed decoupled para-H_2 in a single-moderator configuration. However, due to a more compact design, the STS decoupled moderators still exhibit gains in brightness by a factor of ~3 and ~4 for the para-H_2 and H_2O moderator faces at energies below ~1 eV, relative to the brightness of the FTS decoupled para-H_2 and water moderators, as shown in Figure 8.4 The stationary STS configuration shows slightly better decoupled moderator performance relative to the rotating STS configuration. More information on moderators is provided in references [2] and [3].

Figure 8.1. Coupled para-H_2 moderators; peak brightness versus neutron energy, for the stationary STS (STS-tdr), rotating STS (Rot), and first target station (FTS)

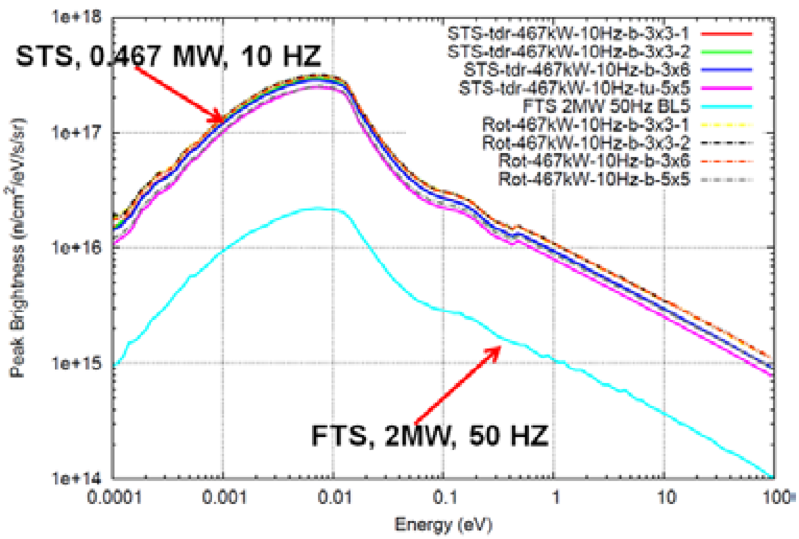

Figure 8.2. Coupled para-H_2 moderators; ratio of the peak brightness of the STS moderators to the peak brightness of the FTS coupled H_2 moderator versus neutron energy

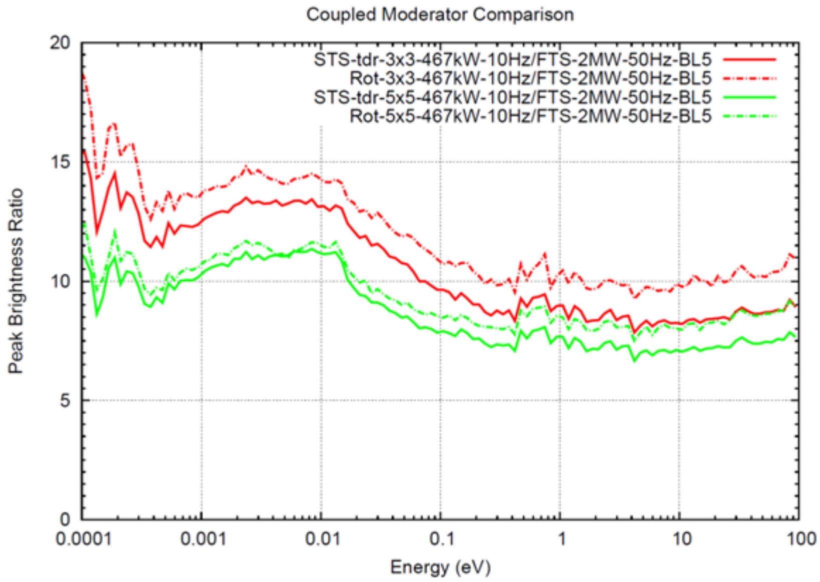

Figure 8.3. Decoupled para-H_2 moderator and ambient temperature H_2O moderator; peak brightness versus neutron energy, for the stationary STS (STS-tdr), rotating STS(Rot), and first target station (FTS)

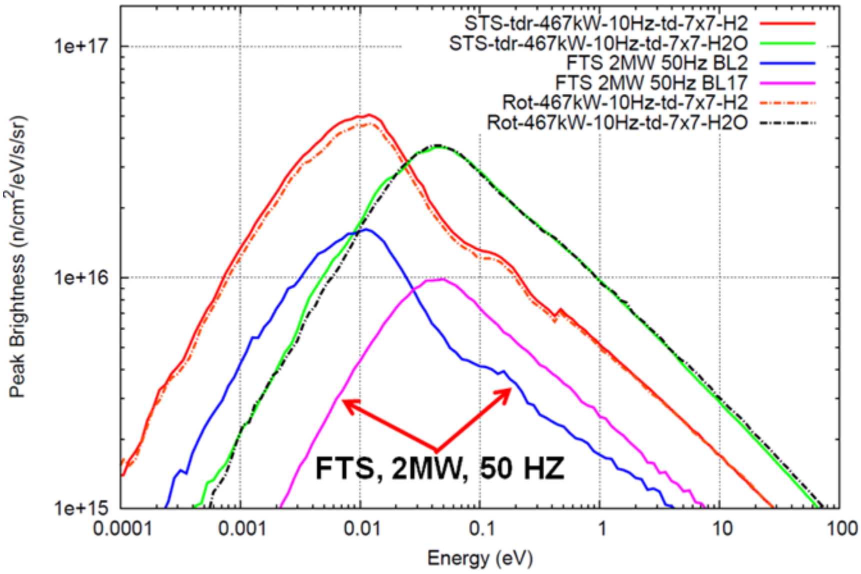

Figure 8.4. Decoupled para-H_2 moderator and ambient temperature H_2O moderator; ratio of the peak brightness of the STS moderators to the peak brightness of the FTS moderators

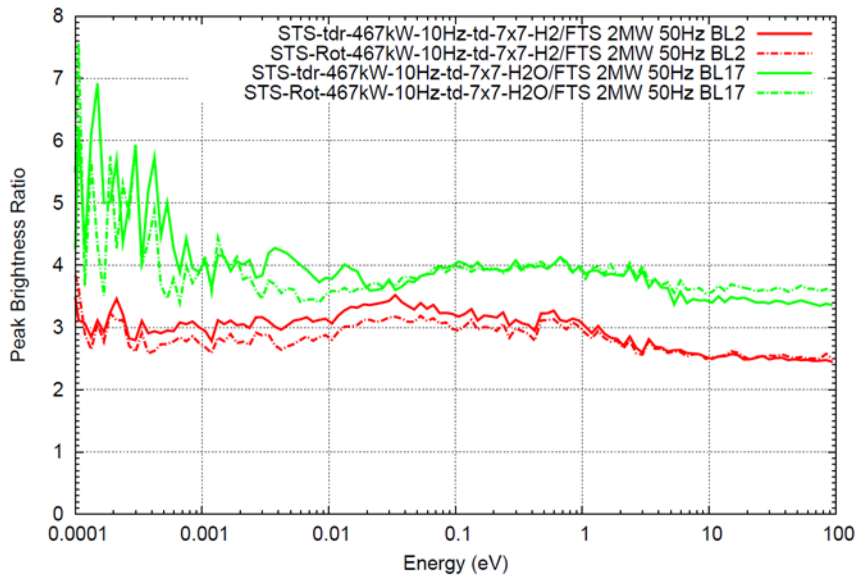

8.3. Energy deposition in the target during operation and decay heat

The compact target design and small proton beam footprint, which are required to achieve high moderator brightness, result in high heating rates in the target during beam on operation and high volumetric density of spallation and activation products which accumulate in the target and are the source of decay heat after the proton beam shutdown.

The distribution of the energy deposition in the rotating target which results from a single proton pulse is illustrated in Figure 8.5. The maximum energy deposition density per pulse in the rotating target is ~80 J/cm^3/pulse, which is about the same as for the stationary target. However, the target rotates and the proton beam energy is spread over much larger volume than in the case of the stationary target. For the water-cooled rotating target, which operates in asynchronous mode, so that the target rotation and beam pulses are not co-ordinated in time, the maximum temperature reaches ~102°C for the beam power of 0.5 MW.

Figure 8.5. Energy deposition in the rotating target resulting from the single proton pulse The peak energy density is ~80 J/cm^3

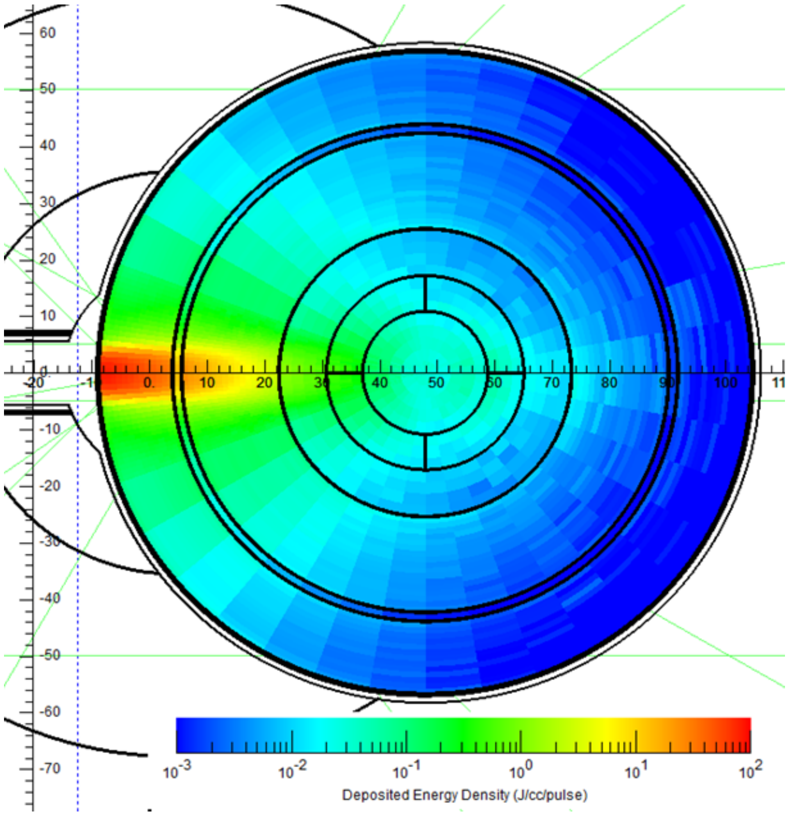

The decay heat versus time after the proton beam shutdown is shown in Figure 8.6 for the stationary and rotating target. For the stationary target after 5 000 hours of continuous operation at 0.470 MW the decay heat is ~ 3.3 kW. The decay heat is confined to a small volume (only ~ 1 400 cm^3) with relatively small surface areas available for cooling. In accident scenarios such as complete loss of active cooling, melting of the target can occur resulting in unacceptable consequences. The rotating target has in fact higher decay heat than the stationary target because it has larger mass and consequently intercepts more radiation. However, thanks to the larger volume, lower decay heat density and larger surface area, the rotating target can withstand loss of active cooling without deterioration. This was the main reason to select rotating target for the STS design baseline, even at the relatively small proton beam power of ~ 0.5 MW.

Figure 8.6. Decay heat versus time following the operation at 0.47 MW for 5 000 hours, for the stationary and rotating target

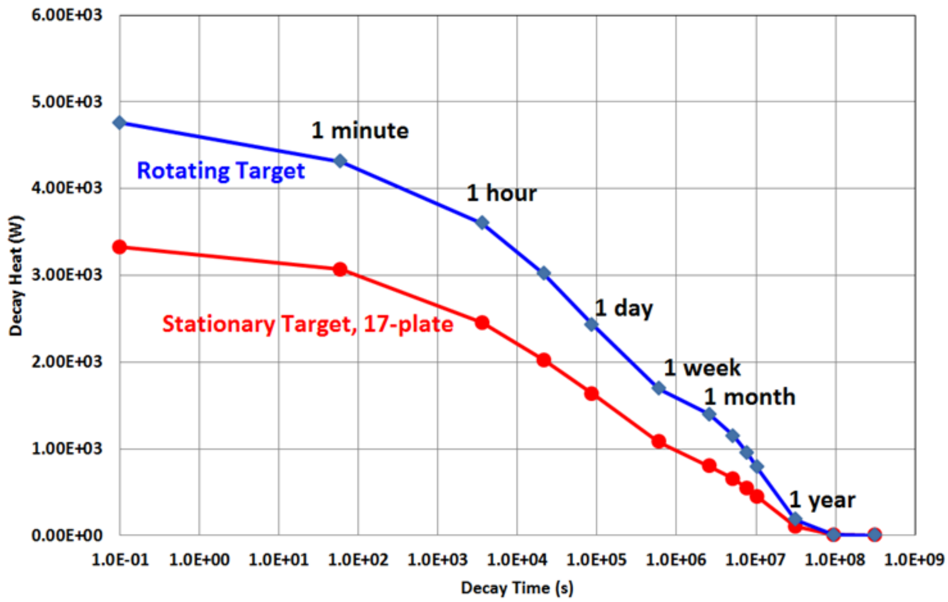

8.4. Shielding analysis for the target monolith

One of the considered target monolith configurations is shown in Figure 8.7. The moderators are embedded in the beryllium reflector, which is surrounded by water-cooled steel, followed by steel and finally enclosed in high density concrete. The analysis was performed entirely with Monte Carlo method. The source was the 1.3 GeV proton beam.

The variance reduction was accomplished with the space and energy-dependant mesh-based weight windows. The weight windows were generated by the ADVANTG methodology [4]. The ADVANTG step of the analysis started with the same MCNPX model that was used for the target and the monolith analysis with MCNPX [5]. However, due to the current limitations of ADVANTG, the proton beam source was replaced with a cell-based neutron source, with the energy spectrum obtained from proton-induced neutron production in the corresponding cell, which was generated in a separate MCNPX run. The forward-weighted consistent adjoint driven importance sampling (FW-CADIS) method was selected for the weight-windows generation, which was developed specifically for multiple tallies and mesh tallies [6]. The FW-CADIS method required two deterministic calculations: an initial forward calculation to estimate the responses and an adjoint calculation to estimate the importance function resulting from the adjoint source. The importance function was then used to construct weight windows. From the MCNPX model of the target and the monolith, ADVANTG generated inputs for the forward and adjoint deterministic calculation with DENOVO [7] as well as the cross-sections for the deterministic calculations, which were constructed from the HILO2K library [8]. Finally the weight-windows file was generated which was applied in the subsequent MCNPX analysis.

Figure 8.7. Vertical section through the target and monolith model

The colours indicate: green –high density concrete, blue –steel, orange – water-cooled steel; the model extent is ~ 12 m across

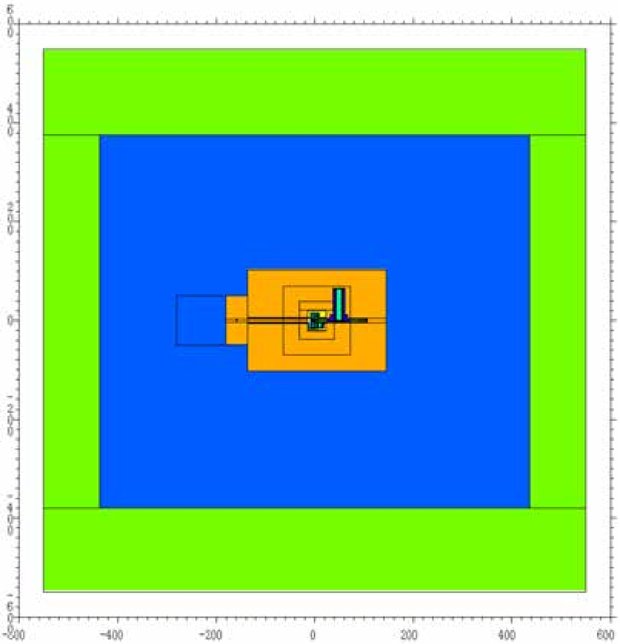

The results are illustrated in Figure 8.8, which shows the neutron and photon dose-rate distribution in the vertical plane through the target monolith. The dose-rate isolines extend further away from the target in the direction of the proton beam, therefore correctly reflecting the predominantly forward directed production of energetic neutron in the target. The asymmetric neutron distribution generates similar asymmetry in the photon dose rate distribution.

Figure 8.9 shows detailed neutron and photon dose-rate distribution along the vertical axis through the target. The monolith provides a peta-scale attenuation of the dose rate, yet the relative standard deviations remain relatively constant and are below 10% over most of the monolith. The extremely high attenuation of radiation through the monolith makes this problem difficult to solve with Monte Carlo method and was traditionally handled with deterministic methods such as discrete ordinates. The analysis presented here was possible only due to utilisation of efficient variance reduction realised with ADVANTG generated energy and space-dependant weight windows.

8.5. Conclusion

This paper presented selected aspects of the neutronics analyses performed for the STS and discussed the performance of the moderators, heating rates, activation analyses and shielding calculations which provide input in the engineering design.

Figure 8.8. Neutron (top) and photon (bottom) dose-rate distribution in the vertical plane through the STS target. The red arrow indicates the direction of the proton beam

The model extent is ~ 12 m across (the scales shown on the edges of the figure are in cm).

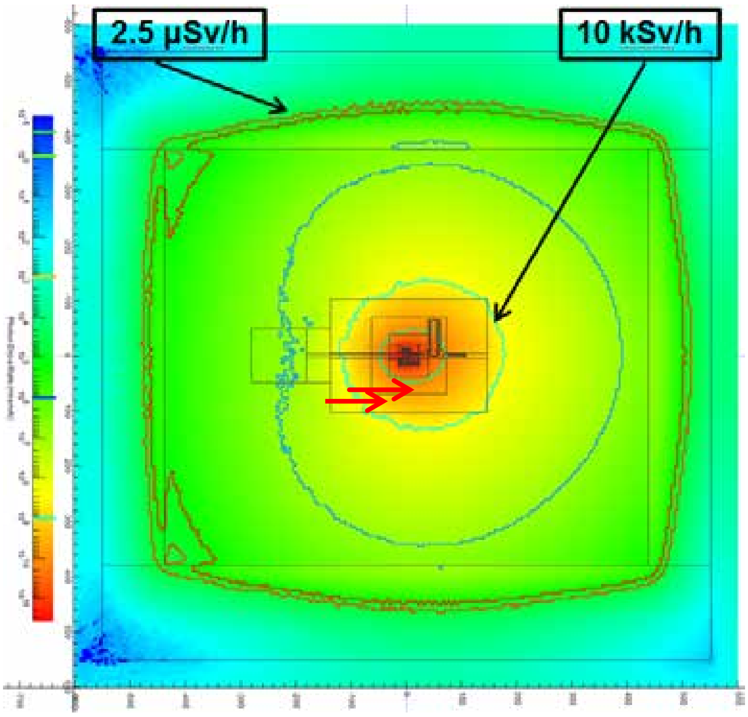

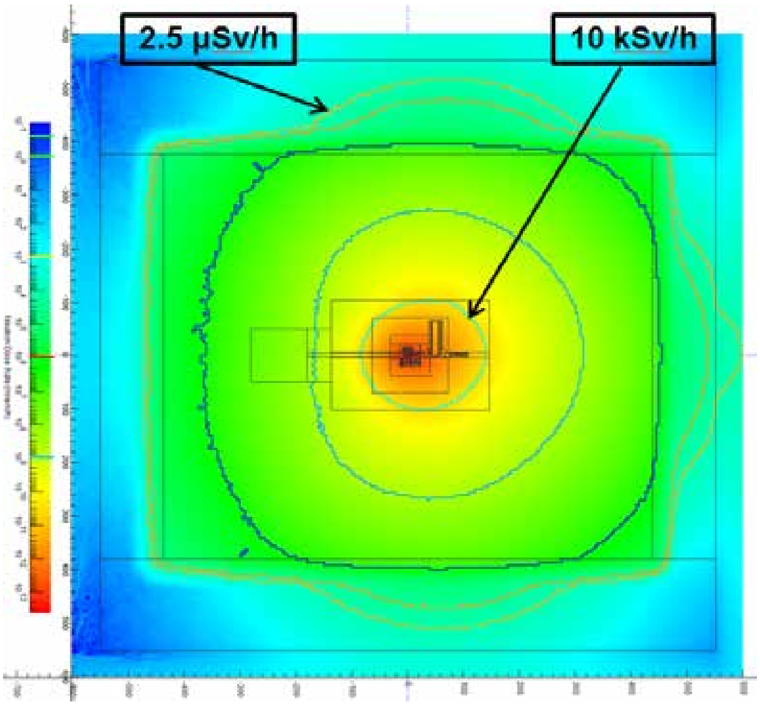

Figure 8.9. Top: neutron and photon dose-rate distributions along the vertical axis through the centre of the top moderator. Relative errors of the neutron and photon dose rates are also shown

Bottom: red line depicts the location of the abscissa of the dose-rate plot on the top

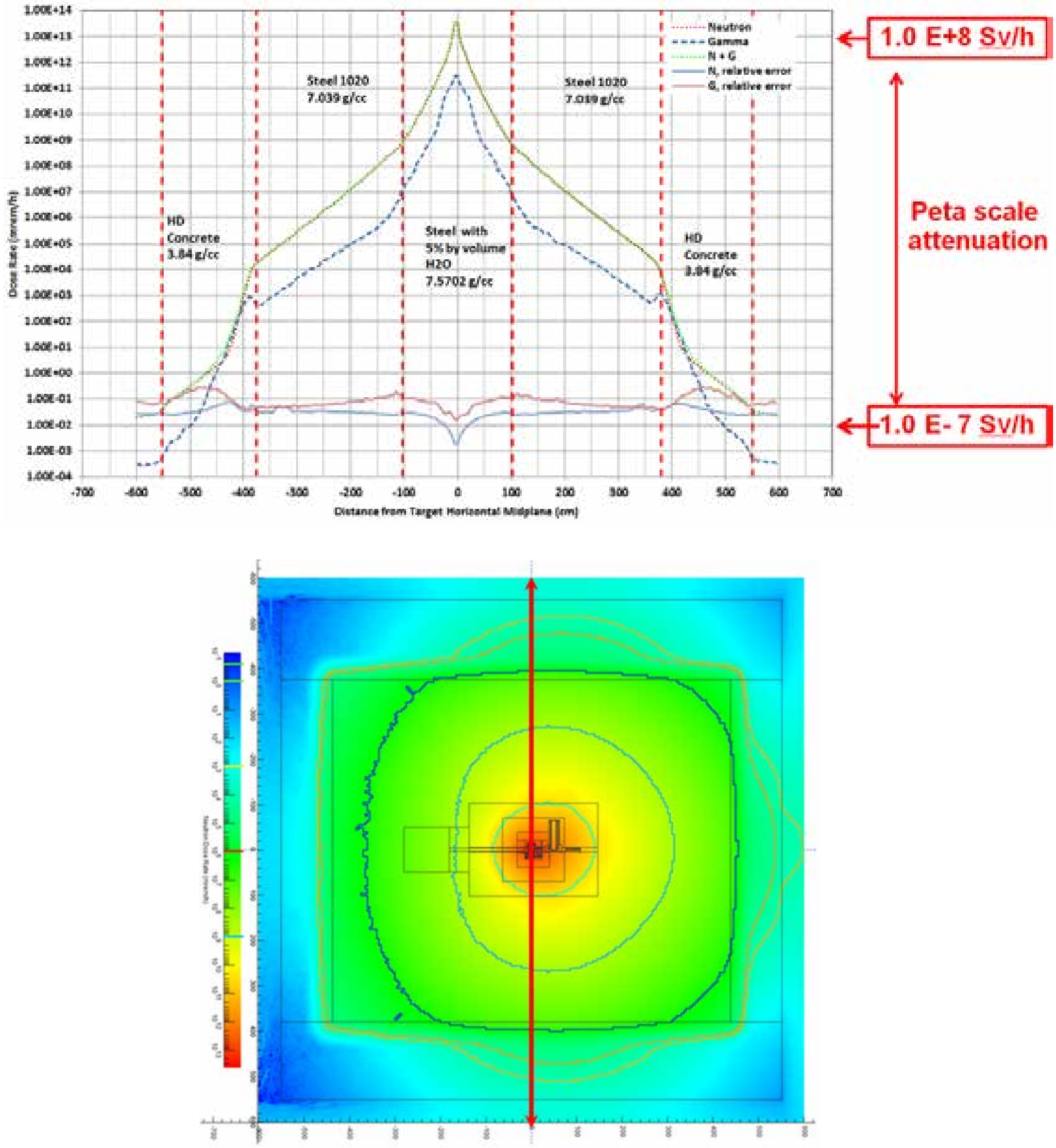

8.6. Acknowledgements

ORNL is managed by UT-Battelle, LLC, under contract DE-AC05-00OR22725 for the US Department of Energy. This research was supported by the DOE Office of Science, Basic Energy Science, Scientific User Facilities.

References

[1] Galambos, J.D. et al. (2015), “Technical Design Report Second Target Station,” ORNL/TM-2015/24, Oak Ridge National Laboratory.

[2] Iverson, E.B. et al. (2014), “Enhancing Neutron Beam Production with a Convoluted Moderator,” *Nucl. Inst. Meth.* A, 762, pp. 31-41.

[3] Gallmeier, F.X. et al (2015), “SNS Second Target Station Moderator Studies,” JAEA-Conf 2015-002, pp. 117-124.

[4] Mosher, S.W. et al. (2015), “ADVANTG—An Automated Variance Reduction Parameter Generator,” ORNL/TM-2013/416 Rev. 1.

[5] Pelowitz, D.B. (2011), “MCNPX User’s Manual Version 2.7.0,” LA-CP-11-00438, Los Alamos National Laboratory.

[6] Wagner, J.C. et al. (2014), “FW-CADIS Method for Global and Regional Variance Reduction of Monte Carlo Radiation Transport Calculations,” *Nucl. Sci. Eng.* 176 (1), pp.37–57.

[7] Evans, T.M. et al. (2010), “Denovo: A New Three-Dimensional Parallel Discrete Ordinates Code in SCALE.” *Nucl. Technol.*, 171 (2), pp. 171–200.

[8] Lillie, R.A. et al. (2001), “HILO2k: Transport Cross-Sections for Neutron Energies to 2 GeV,” Proc. 2001 Amer. Nucl. Soc. Rad. Prot. & Shld. Div. Top. Meet., Santa Fe, NM; RSICC DATA LIBRARY DLC-220.